JACS
JOURNAL OF THE AMERICAN CHEMICAL SOCIETY
pubs.acs.org/JACS
Communication

Dynamic Tuning of the Bandgap of CdSe Quantum Dots through Redox-Active Exciton-Delocalizing N-Heterocyclic Carbene Ligands

Dana E. Westmoreland,[‡] Rafael López-Arteaga,[‡] Leanna Page Kantt, Michael R. Wasielewski, and Emily A. Weiss*

Cite This: J. Am. Chem. Soc. 2022, 144, 4300–4304
Read Online
ACCESS | Metrics & More | Article Recommendations | Supporting Information

ABSTRACT: Ligands that enable the delocalization of excitons beyond the physical boundary of the inorganic core of semiconductor quantum dots (QDs), called "exciton-delocalizing ligands (EDLs)", offer the opportunity to design QD-based environmental sensors with dynamically responsive optical spectra, because the degree of exciton delocalization depends on the electronic structure of the EDL. This paper demonstrates dynamic, reversible tuning of the optical bandgap of a dispersion of CdSe QDs through the redox states of their 1,3-dimesitylnaphthoquinimidazolylidene N-heterocyclic carbene (nqNHC) ligands. Upon binding of the nqNHC ligands to the QD, the optical bandgap bathochromically shifts by up to 102 meV. Electrochemical reduction of the QD-bound nqNHC ligands shifts the bandgap further by up to 25 meV, a shift that is reversible upon reoxidation.

The narrow-line-width optical transitions of semiconductor quantum dots (QDs) and the dramatic shifts in their optical spectra induced by changing the confinement energies of excitonic charge carriers are primary motivations for the development of QD-based ratiometric sensors.[1−4] The traditional methods for changing confinement energy—modifying the composition, shape, and size of the QD—cannot be carried out dynamically and reversibly and therefore are not viable bases for environmental sensing. We have shown that the confinement energy of excitons is also highly sensitive to the adsorption of exciton-delocalizing ligands (EDLs). EDLs allow the wave function of the exciton to extend into the interfacial region, bathochromically shifting the absorption/emission spectra of the QD by up to 1 eV.[5−8] Designing an EDL with an electronic structure that reversibly changes in response to the environment is a means to externally modulate the optical spectra of an EDL-coated QD and an appealing route to ratiometric sensing, but it is a challenge. Extensive mechanistic work has shown that exciton delocalization occurs via significant redistribution of electron density at the QD−ligand interface,[5−11] so we must find external mechanisms to reversibly perturb this electron density to a measurable degree. Such perturbation requires that the site at which the ligand interacts with the environment is conjugated to the site at which it anchors to the QD.

Here, we demonstrate the reversible tuning of the average bandgap of an ensemble of CdSe QDs with applied electrochemical potential through the redox state of an EDL, 1,3-dimesitylnaphthoquinimidazolylidene (nqNHC), an N-heterocyclic carbene. We recently demonstrated that NHCs form stable adlayers of EDLs on CdSe QDs and that varying the (covalent) substituents on the NHC changes the magnitude of exciton delocalization.[12] In this work, we demonstrate a reversible colorimetric response of the QD to an *in situ* modification of the EDL's electronic structure via electrochemical reduction and oxidation. The EDL-coated QD thereby serves as a probe of the local electrochemical potential.

We synthesize 1,3-dimesitylnaphthoquinimidazolium chloride [nqNHC][Cl], where the carbene carbon is protonated, according to a previously published procedure;[13] full details are in the Supporting Information (SI). We modify exchange procedures developed for metal nanoparticles[14−17] to functionalize QDs with the nqNHC ligands (Scheme 1 and Figure S3 of the SI). Our workup procedure includes a postexchange washing step with acetonitrile (ACN) that removes [nqNHC][Cl] decomposition products from the QD solution (Figure

Scheme 1. Ligand Exchange Procedure[a]

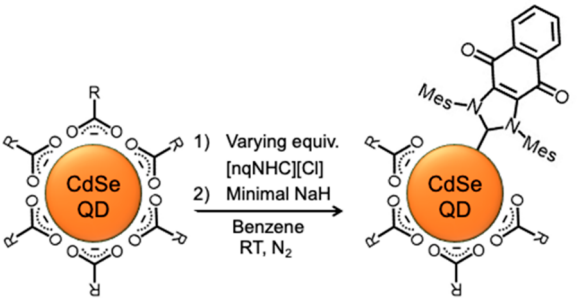

[a]Up to 50 equiv. of [nqNHC][Cl] per QD and 200−300 equiv of NaH per [nqNHC][Cl] are added to 10 μM OA-capped CdSe QDs in benzene.

Received: December 6, 2021
Published: March 7, 2022

https://doi.org/10.1021/jacs.1c12842
J. Am. Chem. Soc. 2022, 144, 4300−4304

S4). ^{1}H NMR analysis shows that nqNHC ligands are bound (Table S1) and that oleate ligands are displaced from the QD surface upon treatment with [nqNHC][Cl] and NaH (Table S2). We detect no residual protonated precursor in dispersions of nqNHC-capped QDs (Figure S5), and the ligand exchange induces no detectable change in the physical size of the particles (Figure S6). All optical and NMR measurements on QD samples are performed using air- and water-free cuvettes or J-Young tubes.

Figure 1A (red) shows that, after treating CdSe QDs (physical radius = 1.2 nm) with 32 equiv of [nqNHC][Cl] through the procedure in Scheme 1, the lowest-energy excitonic absorption peak shifts to lower energy by 102 meV, which, for this size of QD, corresponds to an apparent change in the QD radius (which we denote "ΔR") of 0.15 nm. To most clearly see the shift in the QD absorption, we have subtracted from the "nqNHC-capped QDs" spectrum a broad absorbance of unbound, deprotonated nqNHC centered at 2.07 eV, Figure 1B (blue), and a feature centered at ∼2.75 eV due to absorption from degradation products of [nqNHC][Cl] that appear during ligand exchange (Figures S7 and S8); the primary impurity is the formamide form of [nqNHC][Cl] (Figures S9−S15). The shift of the QD absorption is maintained following our ACN washing procedure (Figure S16). The ΔR that we achieve here with nqNHC-capped QDs is consistent with the values we observed with similar ligands.[12] There is no shift in the optical spectra of QDs treated with either [nqNHC][Cl] alone or NaH alone, and addition of >50 equiv of [nqNHC][Cl] causes minor etching of the QDs (Figures S17 and S18).

Figure 2 demonstrates that we can electrochemically reduce QD-bound nqNHC and shows the reduction potentials of various nqNHC species. This figure includes differential pulse voltammograms (DPVs) of the samples of (i) the protonated [nqNHC][Cl] precursor, (ii) QDs treated with [nqNHC][Cl] but no NaH, and (iii) QDs treated with both [nqNHC][Cl] and NaH. The voltammograms of [nqNHC][Cl] only (Figure 2A) and QDs treated with [nqNHC][Cl] but no NaH (Figure 2B) have peaks corresponding to the reduction potentials of freely diffusing nqNHC at $E_{1/2}$ = −0.8 V and ∼−1.6 V vs. Fc/Fc^{+} (labeled (1) and (4); see Table S3), plus two additional peaks corresponding to the formamide degradation product (labeled (2) and (3); see Figures S7 and S9−15 and Table S3), and one peak that is also present in the "blank" solution of $TBAPF_6$ electrolyte (labeled (5); see Figure S19). The voltammogram for QDs treated with both nqNHC and NaH (Figure 2C) and washed to remove impurities contains one peak (labeled (2); Table S3) corresponding to the reduction of the QD itself (Figure S20), one background peak (labeled (4); Table S3), and two additional peaks (labeled (1) and (3)) with reduction potentials of $E_{1/2}$ = −0.67 V and −1.15 V vs. Fc/Fc^{+} (Table S3), which we assign as the first and second reduction potentials of the deprotonated, QD-bound nqNHC ligands. These results imply that at the open circuit potential (−0.61 V vs. Fc/Fc^{+}) many of the QD-bound nqNHC ligands are already singly reduced.

Figure 1B shows a set of spectra of chemically reduced nqNHC species that aid in our interpretation of the spectra of nqNHC-capped QDs under applied potential. DPV scans of nqNHC-capped QDs that are not washed with ACN (Figure S22 and Table S3) show that, at an applied potential of −1.3 V vs. Fc/Fc^{+}, which is the potential available for chemical reduction by cobaltocene ($CoCp_2$),[18] freely diffusing deproto-

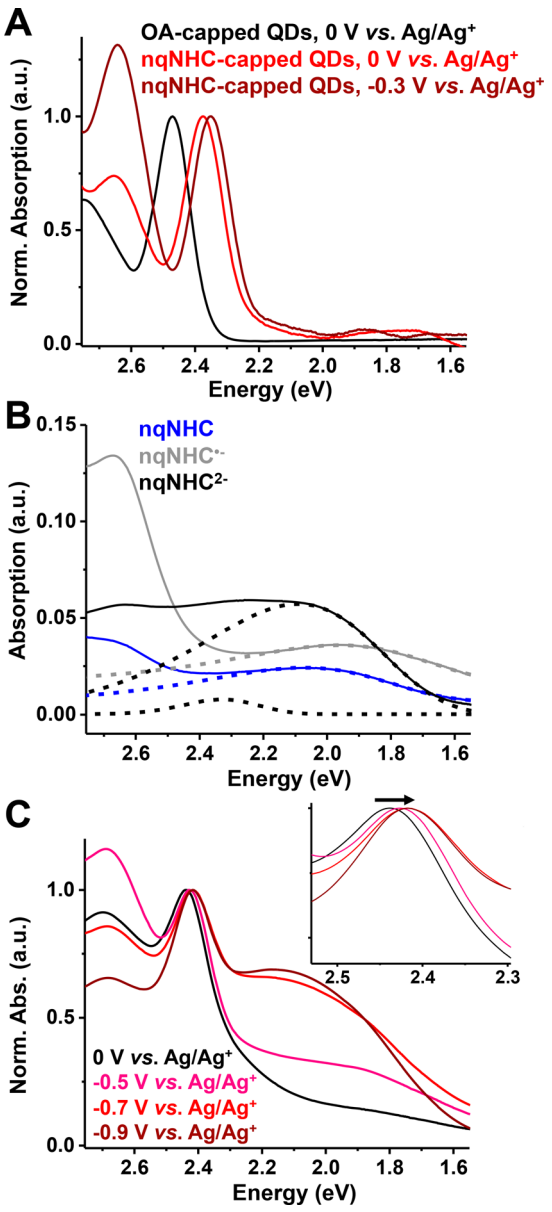

Figure 1. (A) Normalized absorbance spectra of 8.7 μM CdSe QDs in 80:20 (v/v) benzene/ACN and 20 mM $THAPF_6$ electrolyte, capped with oleate (black), and the same QDs treated with 32 equiv of [nqNHC][Cl] plus NaH (red), and the same QDs after bulk electrolysis at an applied potential of −0.3 V vs. Ag/Ag^{+} (dark red). Subtracted from the spectrum of nqNHC-capped QDs at zero potential are the absorbance of deprotonated nqNHC centered at 2.07 eV and a feature centered at ∼2.75 eV due to the degradation product of [nqNHC][Cl]. Subtracted from the spectrum of nqNHC-capped QDs at reductive potential is a linear combination of the spectra of nqNHC$^{\bullet-}$ (44%) and nqNHC^{2-} (56%). Raw spectra are in Figure S8. Subtraction produces an imperfect baseline. (B) Spectra of deprotonated nqNHC (blue), nqNHC$^{\bullet-}$ reduced with 1 equiv of $CoCp_2$ (gray), and nqNHC^{2-} reduced by Na (black), with partial Gaussian fits. (C) Normalized absorbance spectra of 0.15 mM QDs treated with 26 equiv of [nqNHC][Cl] and NaH in 80:20 (v/v) benzene/ACN and 20 mM $THAPF_6$ electrolyte (black) as a function of applied potential. Inset: Zoom-in on the first excitonic peak of the QD. Due to the imprecision of the pseudoreference electrode, the potentials applied in bulk electrolysis, and therefore the degree of reduction of nqNHC achieved, vary from experiment to experiment.

https://doi.org/10.1021/jacs.1c12842
J. Am. Chem. Soc. 2022, 144, 4300−4304

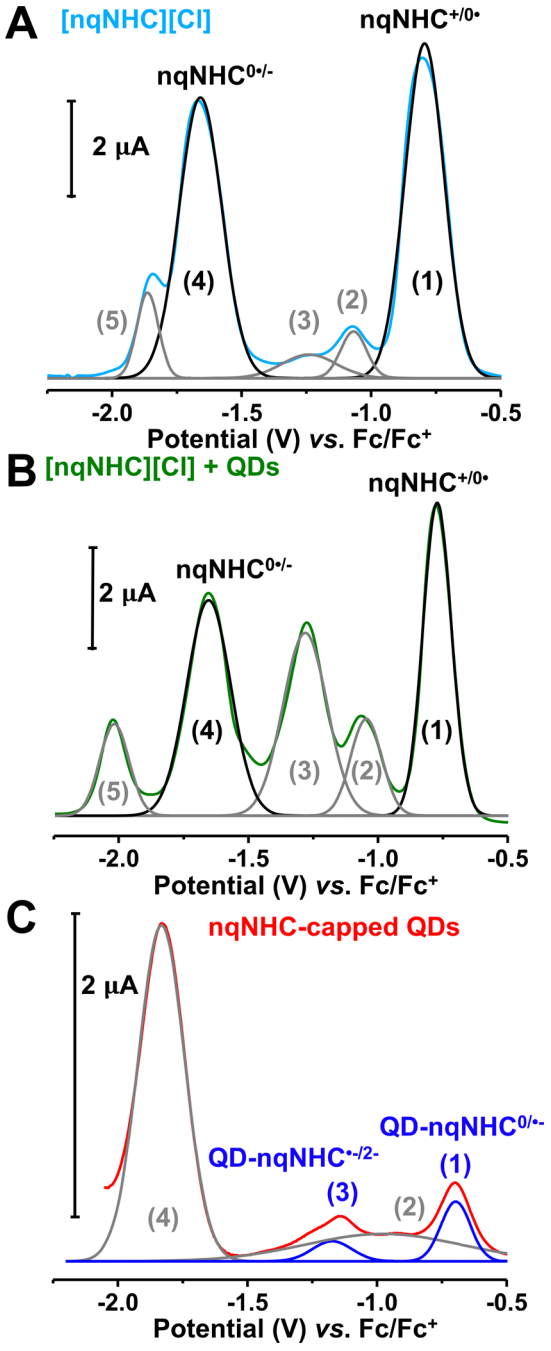

Figure 2. DPVs and multipeak Gaussian fits of (A) 2.7 mM [nqNHC][Cl], (B) 0.08 mM QDs treated with 30 equiv of [nqNHC][Cl] with 60 mM $TBAPF_6$, or (C) 0.08 mM QDs treated with 50 equiv of [nqNHC][Cl] and NaH in 80:20 (v/v) benzene/ACN and washed with ACN to remove degradation products that form during ligand exchange, with 100 mM $THAPF_6$ electrolyte. Peak labels correspond to entries in Table S3.

nated nqNHC should be singly reduced. We therefore know that the additional absorptions present in the spectrum of deprotonated nqNHC in the presence of $CoCp_2$, Figure 1B, gray, are characteristic of $nqNHC^{\bullet-}$. The DPV also shows that, at an applied potential of −3.0 V vs. Fc/Fc^+, the potential available for chemical reduction by Na,[18] the deprotonated freely diffusing nqNHC should be doubly reduced (Figure S22). We therefore assign the additional absorptions present in the spectrum of deprotonated nqNHC in the presence of Na to $nqNHC^{2-}$ (Figure 1B, black).

These assignments allow us to correlate the shift in the QD bandgap to the appearance of reduced nqNHC species upon bulk electrolysis. It is not possible to reference the applied potential to an internal standard such as Fc/Fc^+ without specialized electrodes, so we estimate the applied potential with an Ag/Ag^+ pseudoreference[19,20] and determine the redox state of the nqNHC from the sample's absorbance spectrum, using the spectra in Figure 1B as references. For this reason and because the ligand shells of nqNHC-capped QDs are stabilized by the free molecules in the impurity mixture (Figures S23−S26), we performed the bulk electrolysis experiments on nqNHC-capped QD samples that were not washed with ACN following ligand exchange.

Figure 1A (dark red) shows that, following bulk electrolysis of the nqNHC-capped QDs at −0.3 V vs. Ag/Ag^+, there is a further shift of the QD's excitonic absorption to lower energy by 25 meV (a "$\Delta\Delta R$" of 0.04 nm). This $\Delta\Delta R$ is accompanied by the appearance of an absorption feature centered at 1.96 eV indicative of $nqNHC^{\bullet-}$ and two absorption features centered at 2.09 and 2.33 eV indicative of $nqNHC^{2-}$. We subtracted these features from the spectrum in Figure 1A using the fits of independently measured spectra of reduced nqNHC species in Figure 1B to more clearly show the shift of the QD exciton peak, but they are seen in the raw spectra in Figure S27. Figure 1C shows the progressive shift of the QD exciton peak with accompanying evolution of the features of the reduced nqNHC species. We only observe this additional bathochromic shift of the QD spectrum under applied potential when the nqNHC is present *and* bound to the QD surface (Figure S28). These data imply that the observed $\Delta\Delta R$ in the optical spectra of the QD in Figure 1A,C are due to a change in redox state of the bound nqNHC ligand to its dianionic state. The additional bathochromic shift saturates upon applying an electrochemical potential, at which 46% of the freely diffusing nqNHC is singly reduced and 54% is doubly reduced (Figure S29). This result is reasonable given that, according to the DPV (Figure S22), a potential reductive enough to doubly reduce the QD-bound nqNHC produces both singly and doubly reduced freely diffusing nqNHC.

Figure 3 shows that the $\Delta\Delta R$ is reversible upon its reoxidation. This figure includes the initial ground state absorbance spectrum of nqNHC-capped QDs at the open circuit potential, with contributions from the QDs and deprotonated, neutral nqNHC (Figure S30A). The initial ΔR relative to the oleate-capped QDs (spectrum not shown) is 65 meV. Following bulk electrolysis of the nqNHC-capped QD solution at −0.9 V vs. Ag/Ag^+, we measure an additional bathochromic shift of 21 meV ($\Delta\Delta R$ = 0.025 nm) (red) and contributions to the spectrum from $nqNHC^{\bullet-}$ (38%) and $nqNHC^{2-}$ (62%; Figure S30B). We then perform electrolysis at +0.5 V vs. Ag/Ag^+ (Figure 3, blue), which reoxidizes the reduced nqNHC species. The QD peak returns to its initial, postexchange, position, and the absorptions of reduced nqNHC species disappear.

In summary, we have demonstrated that the redox-active EDL nqNHC is a handle by which we can externally and reversibly tune the bandgap of CdSe QDs through applied potential. The additional exciton delocalization produced by reduction of QD-bound nqNHC, although small, is clearly measurable and reversible with reoxidation. This work therefore demonstrates dynamic control of the quantum

https://doi.org/10.1021/jacs.1c12842
J. Am. Chem. Soc. 2022, 144, 4300−4304

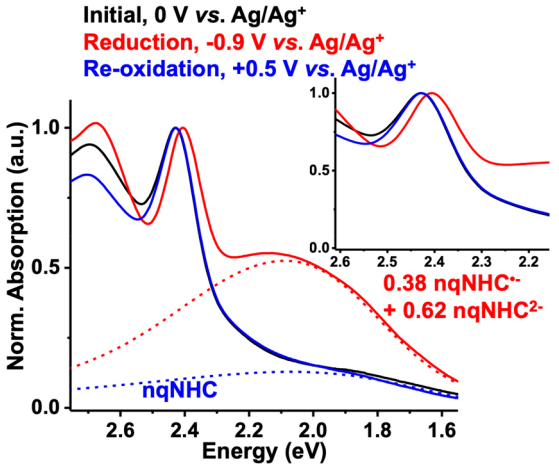

Figure 3. Normalized absorbance spectra of QDs treated with 26 equiv of [nqNHC][Cl] and NaH (black), and the same sample after (i) bulk electrolysis at a potential of −0.9 V vs. Ag/Ag^+ (red), and then (ii) bulk electrolysis at a potential of +0.5 V vs. Ag/Ag^+ (blue), and partial Gaussian fits using independently measured spectra of nqNHC species. Samples are in 80:20 (v/v) benzene/ACN and contain 20 mM $THAPF_6$ electrolyte. Inset: Zoom-in on the excitonic peak.

confinement of a QD's exciton through its ligands and the local potential, which is tunable *in situ*.[5−7,9,10,12] We also contribute a new procedure for exchanging a QD's native ligands for NHCs that is generalizable to other NHC-based ligands.[12,21]

Our results present a simple optical strategy for dynamically sensing changes to the electrochemical potential of a solution. Notably, the optical response of the QDs to the local potential is instantaneous (upon change in redox state of the EDL) and can, in principle, be realized throughout the visible and near-infrared using other QD materials.[6] Unlike Förster resonance energy transfer (FRET)-based sensing strategies, an EDL-based sensor does not require the presence of two chromophores with overlapping optical spectra, which can complicate quantitative interpretation of such systems.[1,22−32] Such a sensor would require deposition and stabilization of the nqNHC-capped QDs into a solid film, as has been achieved with photoswitchable NHC derivatives.[33,34] The large library of synthetic procedures for functionalizing NHCs[35−37] makes them excellent scaffolds for designing analyte-specific sensors.

■ ASSOCIATED CONTENT

Supporting Information

The Supporting Information is available free of charge at https://pubs.acs.org/doi/10.1021/jacs.1c12842.

Details of QD and [nqNHC][Cl] syntheses, ^1H NMR experiments, ground state spectroscopy experiments, and electrochemical experiments, including Figures S1−S31 and Tables S1−S3 (PDF)

■ AUTHOR INFORMATION

Corresponding Author

Emily A. Weiss − *Department of Chemistry, Northwestern University, Evanston, Illinois 60208-3113, United States;* orcid.org/0000-0001-5834-463X; Email: e-weiss@northwestern.edu

Authors

Dana E. Westmoreland − *Department of Chemistry, Northwestern University, Evanston, Illinois 60208-3113, United States*

Rafael López-Arteaga − *Department of Chemistry, Northwestern University, Evanston, Illinois 60208-3113, United States;* orcid.org/0000-0001-8058-3469

Leanna Page Kantt − *Department of Chemistry, Northwestern University, Evanston, Illinois 60208-3113, United States*

Michael R. Wasielewski − *Department of Chemistry, Northwestern University, Evanston, Illinois 60208-3113, United States;* orcid.org/0000-0003-2920-5440

Complete contact information is available at: https://pubs.acs.org/10.1021/jacs.1c12842

Author Contributions

‡D.E.W. and R.L.-A. contributed equally.

Notes

The authors declare no competing financial interest.

■ ACKNOWLEDGMENTS

This work was primarily funded by the Air Force Office of Scientific Research (AFOSR, grant number FA9550-20-1-0364). The authors also received support from the National Institutes of Health (grant no. R21GM127919) and the National Science Foundation under Award CHE-1925690 (M.R.W.). We utilized instrumentation in the IMSERC facility at Northwestern University, which has received support from the Soft and Hybrid Nanotechnology Experimental Resource (NSF ECCS-1542205), the NIH (1S10OD012016-01/1S10RR019071-01A1), the state of Illinois, and the International Institute for Nanotechnology (IIN). This work made use of the EPIC facilities of Northwestern University's NUANCE Center. We thank Dr. Mark Maskeri for providing materials for preliminary experiments and David D. Xu for assistance with STEM image collection.

■ REFERENCES

(1) Medintz, I. L.; Clapp, A. R.; Mattoussi, H.; Goldman, E. R.; Fisher, B.; Mauro, J. M. Self-assembled nanoscale biosensors based on quantum dot FRET donors. *Nat. Mater.* **2003**, *2* (9), 630−638.

(2) Bruchez, M.; Moronne, M.; Gin, P.; Weiss, S.; Alivisatos, A. P. Semiconductor Nanocrystals as Fluorescent Biological Labels. *Science* **1998**, *281* (5385), 2013−2016.

(3) Gerion, D.; Pinaud, F.; Williams, S. C.; Parak, W. J.; Zanchet, D.; Weiss, S.; Alivisatos, A. P. Synthesis and Properties of Biocompatible Water-Soluble Silica-Coated CdSe/ZnS Semiconductor Quantum Dots. *J. Phys. Chem. B* **2001**, *105* (37), 8861−8871.

(4) Dabbousi, B. O.; Rodriguez-Viejo, J.; Mikulec, F. V.; Heine, J. R.; Mattoussi, H.; Ober, R.; Jensen, K. F.; Bawendi, M. G. (CdSe)ZnS Core−Shell Quantum Dots: Synthesis and Characterization of a Size Series of Highly Luminescent Nanocrystallites. *J. Phys. Chem. B* **1997**, *101* (46), 9463−9475.

(5) Frederick, M. T.; Weiss, E. A. Relaxation of Exciton Confinement in CdSe Quantum Dots by Modification with a Conjugated Dithiocarbamate Ligand. *ACS Nano* **2010**, *4* (6), 3195−3200.

(6) Frederick, M. T.; Amin, V. A.; Cass, L. C.; Weiss, E. A. A Molecule to Detect and Perturb the Confinement of Charge Carriers in Quantum Dots. *Nano Lett.* **2011**, *11* (12), 5455−5460.

(7) Frederick, M. T.; Amin, V. A.; Swenson, N. K.; Ho, A. Y.; Weiss, E. A. Control of Exciton Confinement in Quantum Dot−Organic Complexes through Energetic Alignment of Interfacial Orbitals. *Nano Lett.* **2013**, *13* (1), 287−292.

(8) Amin, V. A.; Aruda, K. O.; Lau, B.; Rasmussen, A. M.; Edme, K.; Weiss, E. A. Dependence of the Band Gap of CdSe Quantum Dots on the Surface Coverage and Binding Mode of an Exciton-Delocalizing Ligand, Methylthiophenolate. *J. Phys. Chem. C* **2015**, *119* (33), 19423−19429.
(9) Jin, S.; Harris, R. D.; Lau, B.; Aruda, K. O.; Amin, V. A.; Weiss, E. A. Enhanced rate of radiative decay in cdse quantum dots upon adsorption of an exciton-delocalizing ligand. *Nano Lett.* **2014**, *14* (9), 5323−5328.
(10) Harris, R. D.; Amin, V. A.; Lau, B.; Weiss, E. A. Role of interligand coupling in determining the interfacial electronic structure of colloidal CdS quantum dots. *ACS Nano* **2016**, *10* (1), 1395−1403.
(11) Aruda, K. O.; Amin, V. A.; Thompson, C. M.; Lau, B.; Nepomnyashchii, A. B.; Weiss, E. A. Description of the Adsorption and Exciton Delocalizing Properties of p-Substituted Thiophenols on CdSe Quantum Dots. *Langmuir* **2016**, *32* (14), 3354−3364.
(12) Westmoreland, D. E.; López-Arteaga, R.; Weiss, E. A. N-Heterocyclic Carbenes as Reversible Exciton-Delocalizing Ligands for Photoluminescent Quantum Dots. *J. Am. Chem. Soc.* **2020**, *142* (5), 2690−2696.
(13) Tennyson, A. G.; Lynch, V. M.; Bielawski, C. W. Arrested Catalysis: Controlling Kumada Coupling Activity via a Redox-Active N-Heterocyclic Carbene. *J. Am. Chem. Soc.* **2010**, *132* (27), 9420−9429.
(14) Ranganath, K. V. S.; Kloesges, J.; Schäfer, A. H.; Glorius, F. Asymmetric Nanocatalysis: N-Heterocyclic Carbenes as Chiral Modifiers of Fe3O4/Pd nanoparticles. *Angew. Chem., Int. Ed.* **2010**, *49* (42), 7786−7789.
(15) Richter, C.; Schaepe, K.; Glorius, F.; Ravoo, B. J. Tailor-made N-heterocyclic carbenes for nanoparticle stabilization. *Chem. Commun.* **2014**, *50* (24), 3204−3207.
(16) Ferry, A.; Schaepe, K.; Tegeder, P.; Richter, C.; Chepiga, K. M.; Ravoo, B. J.; Glorius, F. Negatively Charged N-Heterocyclic Carbene-Stabilized Pd and Au Nanoparticles and Efficient Catalysis in Water. *ACS Catal.* **2015**, *5* (9), 5414−5420.
(17) Tegeder, P.; Freitag, M.; Chepiga, K. M.; Muratsugu, S.; Möller, N.; Lamping, S.; Tada, M.; Glorius, F.; Ravoo, B. J. N-Heterocyclic Carbene-Modified Au−Pd Alloy Nanoparticles and Their Application as Biomimetic and Heterogeneous Catalysts. *Chem. Eur. J.* **2018**, *24* (70), 18682−18688.
(18) Connelly, N. G.; Geiger, W. E. Chemical Redox Agents for Organometallic Chemistry. *Chem. Rev.* **1996**, *96* (2), 877−910.
(19) Bard, A. J.; Faulkner, L. R. *Electrochemical Methods: Fundamentals and Applications*, 2nd ed.; John Wiley & Sons, Inc., 2001; pp 53−54, 417−423.
(20) Booman, G. L.; Holbrook, W. B. Electroanalytical Controlled-Potential Instrumentation. *Anal. Chem.* **1963**, *35* (12), 1793−1809.
(21) Du, L.; Nosratabad, N. A.; Jin, Z.; Zhang, C.; Wang, S.; Chen, B.; Mattoussi, H. Luminescent Quantum Dots Stabilized by N-Heterocyclic Carbene Polymer Ligands. *J. Am. Chem. Soc.* **2021**, *143* (4), 1873−1884.
(22) Snee, P. T.; Somers, R. C.; Nair, G.; Zimmer, J. P.; Bawendi, M. G.; Nocera, D. G. A Ratiometric CdSe/ZnS Nanocrystal pH Sensor. *J. Am. Chem. Soc.* **2006**, *128* (41), 13320−13321.
(23) Shamirian, A.; Samareh Afsari, H.; Hassan, A.; Miller, L. W.; Snee, P. T. Vitro Detection of Hypoxia Using a Ratiometric Quantum Dot-Based Oxygen Sensor. *ACS Sens* **2016**, *1* (10), 1244−1250.
(24) Jin, T.; Sasaki, A.; Kinjo, M.; Miyazaki, J. A quantum dot-based ratiometric pH sensor. *Chem. Commun.* **2010**, *46* (14), 2408−2410.
(25) Susumu, K.; Field, L. D.; Oh, E.; Hunt, M.; Delehanty, J. B.; Palomo, V.; Dawson, P. E.; Huston, A. L.; Medintz, I. L. Purple-, Blue-, and Green-Emitting Multishell Alloyed Quantum Dots: Synthesis, Characterization, and Application for Ratiometric Extracellular pH Sensing. *Chem. Mater.* **2017**, *29* (17), 7330−7344.
(26) Willard, D. M.; Carillo, L. L.; Jung, J.; Van Orden, A. CdSe−ZnS Quantum Dots as Resonance Energy Transfer Donors in a Model Protein−Protein Binding Assay. *Nano Lett.* **2001**, *1* (9), 469−474.
(27) Tran, P. T.; Anderson, G. P.; Mauro, J. M.; Mattoussi, H. Use of Luminescent CdSe−ZnS Nanocrystal Bioconjugates in Quantum Dot-Based Nanosensors. *Phys. Status Solidi B* **2002**, *229* (1), 427−432.
(28) Clapp, A. R.; Medintz, I. L.; Mauro, J. M.; Fisher, B. R.; Bawendi, M. G.; Mattoussi, H. Fluorescence Resonance Energy Transfer Between Quantum Dot Donors and Dye-Labeled Protein Acceptors. *J. Am. Chem. Soc.* **2004**, *126* (1), 301−310.
(29) Medintz, I. L.; Mattoussi, H. Quantum dot-based resonance energy transfer and its growing application in biology. *Phys. Chem. Chem. Phys.* **2009**, *11* (1), 17−45.
(30) Medintz, I. L.; Uyeda, H. T.; Goldman, E. R.; Mattoussi, H. Quantum dot bioconjugates for imaging, labelling and sensing. *Nat. Mater.* **2005**, *4* (6), 435−446.
(31) Zhang, C.-Y.; Yeh, H.-C.; Kuroki, M. T.; Wang, T.-H. Single-quantum-dot-based DNA nanosensor. *Nat. Mater.* **2005**, *4* (11), 826−831.
(32) Moroz, P.; Jin, Z.; Sugiyama, Y.; Lara, D. A.; Razgoniaeva, N.; Yang, M.; Kholmicheva, N.; Khon, D.; Mattoussi, H.; Zamkov, M. Competition of Charge and Energy Transfer Processes in Donor−Acceptor Fluorescence Pairs: Calibrating the Spectroscopic Ruler. *ACS Nano* **2018**, *12* (6), 5657−5665.
(33) Nguyen, D. T.; Freitag, M.; Gutheil, C.; Sotthewes, K.; Tyler, B. J.; Böckmann, M.; Das, M.; Schlüter, F.; Doltsinis, N. L.; Arlinghaus, H. F.; Ravoo, B. J.; Glorius, F. An Arylazopyrazole-Based N-Heterocyclic Carbene as a Photoswitch on Gold Surfaces: Light-Switchable Wettability, Work Function, and Conductance. *Angew. Chem., Int. Ed.* **2020**, *59* (32), 13651−13656.
(34) Dery, S.; Alshanski, I.; Mervinetsky, E.; Feferman, D.; Yitzchaik, S.; Hurevich, M.; Gross, E. The influence of surface proximity on photoswitching activity of stilbene-functionalized N-heterocyclic carbene monolayers. *Chem. Commun.* **2021**, *57* (51), 6233−6236.
(35) Smith, C. A.; Narouz, M. R.; Lummis, P. A.; Singh, I.; Nazemi, A.; Li, C.-H.; Crudden, C. M. N-Heterocyclic Carbenes in Materials Chemistry. *Chem. Rev.* **2019**, *119* (8), 4986−5056.
(36) Huynh, H. V. Electronic Properties of N-Heterocyclic Carbenes and Their Experimental Determination. *Chem. Rev.* **2018**, *118* (19), 9457−9492.
(37) Hopkinson, M. N.; Richter, C.; Schedler, M.; Glorius, F. An overview of N-heterocyclic carbenes. *Nature* **2014**, *510* (7506), 485−496.

https://doi.org/10.1021/jacs.1c12842
J. Am. Chem. Soc. 2022, 144, 4300−4304